

VOID FRACTION & BUBBLE DISTRIBUTION MEASUREMENT IN BUBBLE COLUMN REACTOR

**FINAL YEAR PROJECT-1
BY PRANESH KUMAR SAHA
BME-IV ROLL-001511201113
GUIDE:PROF. SOURAV SARKAR**

Introduction

Two phase flow is used in many chemical reactors. One of the simplest and widely used of them is the bubble column reactor. Bubble column reactors belong to the general class of multiphase reactors which consist of three main categories namely, the trickle bed reactor (fixed or packed bed), fluidized bed reactor, and the bubble column reactor. It operates with gas-liquid mixture and consists of vertically arranged columns filled with liquid, at the bottom of which gas is inserted. A perforated plate called sparger is present and breaks down the gas introduced into small bubbles, thus the name. This leads to increase in surface area for heat and mass transfer.

The bubble column reactor is very important tool in a variety of industries like chemical, petrochemical, biochemical and metallurgical. They are used especially in chemical reactions involving reactions such as oxidation, chlorination, alkylation, polymerization and hydrogenation, in the gas conversion processes and in fermentation and biological wastewater treatment. Some other chemical applications are the indirect coal liquefaction process to produce transportation fuel, methanol synthesis and manufacture other synthetic fuels.

Industrial bubble columns usually operate with a length-to-diameter ratio, or aspect ratio of at least 5. In biochemical applications this value usually varies between 2 and 5.

Advantages of bubble column reactor:

1. They provide advantages both in design and operation as compared to other reactors.
2. They have excellent heat and mass transfer characteristics.
3. Little maintenance and low operating cost.
4. Compactness and less moving parts.

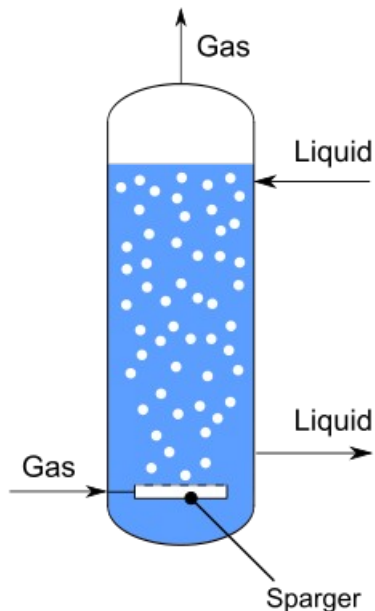


Fig 1: Bubble Column Reactor

The design and scale-up of bubble column reactors generally depend on the quantification of three main phenomena: (i) heat and mass transfer characteristics; (ii) mixing characteristics; (iii) chemical kinetics of the reacting system.

The main parameters affecting the design of bubble column reactors are the specific gas-liquid interfacial area, Sauter mean bubble diameter, heat transfer coefficient, physio-chemical properties and gas hold-up.

We can note that in most of the properties the bubble size or diameter is of much importance. The reaction in bubble column reactor takes place through the surface of the bubbles of the gaseous

phase. The design and scale of a bubble column reactor depends on the transportation coefficients which depend on bubble size and spatial distribution of bubbles (local void fraction). The bubble size also affects the holdup factor which in turn affects the reaction rate and efficiency of the reactor. Gas holdup is a dimensionless parameter which characterizes the transport phenomenon of the reactor. It is basically the volume fraction of the gas phase occupied by the gas bubbles. So, the study of bubble size and thus void fraction variation with change in flow characteristics is of utmost importance in understanding the effect of those characteristics on the overall reaction rate and efficiency of the reactor. One of the important flow characteristics is the superficial gas velocity which in turn depends on the gaseous phase flow rate. Therefore, the study of the variation of bubble diameter (and void fraction) with gas phase flowrate is very important.

Literature Review

Over the years many papers have been published on the quantisation of bubbles and void fraction in bubble column reactors. In (10) dynamic gas disengagement process with the help of pressure transducers to measure the liquid level drop is employed to quantify gas holdup and calculate the sauter mean bubble diameter. This method is based on pressure and temperature sensors and was before the advent of modern cheap computational power. During the 2000's a gradual change to imaging based techniques for quantification of bubbles is observed due to the advent of new cheap and better imaging sensors and as well as personal computers in laboratories providing cheap computation. In (9) an image analysis based algorithm based on the famous watershed technique is proposed to segment the bubbles and measure the void fraction for overlapped bubbles. Similarly in (7) both holdup measurement and bubble size determination is done. Holdup measurement is done for hydrodynamics study. Image analysis technique also used in this paper and simple thresholding is used. In (6) voidage probes are used for void fraction measurements. The image analysis based experiments have all used high speed cameras. In (2) gamma ray densitometry has been employed to determine the axial and radial distribution of void fraction and a high speed camera with borescope is used for determining variation of bubble size.

In most of this cases the microbubbles has been considered and generally development of suitable image processing techniques for accurate detection and quantification of bubbles have been looked over by considering bubbles of mostly uniform size or by employing very costly imaging techniques. But in industrial conditions such a costly setup has hindered the use of above methods for control and build-up of column reactors. So in this project we have developed a very flexible, computationally inexpensive and robust algorithm for bubble detection and quantification.

The contributions of this project are as follows:

1. A new image segmentation and grouping technique for occluded and noisy bubble images.
2. An entirely new bubble quantification image processing algorithm is proposed and tested.
3. Study of the variation of bubble size and void fraction at differennt flow rates of air

Experimental Setup

The experimental setup has the following components:

1. Glass cylindrical column
2. Two rotometers- one for water and another for air. First one is connected towards the bottom right corner and the second one at top left corner
3. One air compressor

4. One water pump
5. One steel tank
6. Led lights
7. Paper as diffuser

The experiment involves only the use of air circuit for injecting air inside the cylinder. The water circuit may be used to induce an opposite flow in the water which increases the rate of reaction. Picture is taken at ten different values of air flow rate. Firstly the glass column is filled completely with water by using the water pump. After the water has filled the tube the pump is shut down and the compressor is connected. After switching on the compressor the air flow rate is controlled by the help of the rotometer and varying the speed of compressor. When the desired volume flow rate is obtained the system is given some time to stabilise. This is done to ensure steady flow conditions have been attained. Then the picture of the bubbles is taken with help of Nikon camera.



Fig 2: Experimental Setup



Fig 3: ROTOMETER



Fig 4: STEEL TANK

Algorithm:

The algorithm developed has the following major steps:

1. Image segmentation
2. Thinning of segmented image
3. Unwanted segment cleansing
4. Marking of connected components
5. Grouping and selection
6. Curve fitting

The input color image is first converted to greyscale by using the following formulae:

Then the grey scale image is convolved with a 3x3 gaussian kernel for smoothening out the low level noises in the image.

This smoothed out image is then passed on to the segmentation algorithm.

1. Local adaptive resonance based image binarisation

In designing the algorithm for the segmentation the main aim was to keep it as computationally inexpensive as possible. But normal segmentation methods like Canny edge detector and Watershed algorithm gave inaccurate results owing to fact that a lot of shadows in the background. It was observed that the shadow pixels had very similar grey level values as the bubble boundaries. Also, the inside areas of bubbles themselves suffered from the effect of shadowing. For this setup of noise it becomes very important to consider the effect the pixels have on each other. If we think about human vision we can very easily identify the connectivity between pixels to extract meaningful structure even in presence of large amounts of noise.

The resonance algorithm as proposed in various papers (Dai,Zhao and Zhao,2007; He and Chen,2000) is based on emphasizing the similarity between neighbouring pixels and carrying it forward. This eliminates any effect of shadowing in the background as any gradual change in pixel value is neglected and only sudden changes are recorded as boundary between adjacent regions. A threshold μ is defined as the distance metric and a mapping of two points a & b $P(a,b)$ gives the distance between two adjacent neighbouring pixels. If $P(a,b)$ is less than μ then b belongs to same class as a , else it marks a boundary. The point at which a new region starts is called a seed point.

In resonance algorithm 3 aspects are very important:

1. One or several seed points,
2. The features to determine the difference between points,
3. The parameter of the threshold δ .

In previous papers no definitive method of selection of delta has been proposed. Also in this application we found that the background region was a continuous region and should be identified as one entity. But direct application of resonance algorithm although removes background shadowing divides the background into regions as there is substantial grey level value change. So the main motive was to automate the threshold value selection and maintain continuity in background.

It was observed that selecting a global threshold even for resonance algorithm is inefficient. Therefore the threshold was taken as :

$$\text{Threshold} = \mu = (\text{Max}(I_{\text{smooth}}[i]) - \text{mean}(I_{\text{smooth}}) - (\text{Min}(I_{\text{smooth}}[i]) - \text{mean}(I_{\text{smooth}}))) / 2 + C_1$$

where $I_{\text{smooth}}[i]$ denotes a row of the smoothed image.

The threshold gives a value for each row such that in local condition whether a pixel is background or foreground can be determined.

A second threshold μ_2 defined for this kernel as:

$$\text{Thresh}_2 = \mu_2 = \text{Mean}(K) + C_2$$

where K is a 7×7 kernel centered at (i,j) and C_2 is constant.

For every pixel position in I_{smooth} (i,j) we take a 7×7 neighbourhood centered at (i,j) . Then the μ_2 is used to determine whether the pixel is foreground or background. This removes the effect of localised variation of pixel value with position.

After determining the nature of the mid-pixel all the other pixel values are assigned to either foreground or background depending on the difference in magnitude from the midpixel and threshold μ .

Thus we propose a modified resonance algorithm based on adaptive thresholding of the seed pixel. The output after this thresholding is transformed through opening operation.

The algorithm is as given below:

Steps

mid := mean(I_{smooth})

[max]_{N X 1} := Max in each row([I_{smooth}]_{N X N} - [1]_{N X N} * mid |)

$[min]_{N \times 1} := \text{Max in each row}([I_{\text{smooth}}]_{N \times N}, [1]_{N \times N} * \text{mid})$
 $[thresh1]_{N \times 1} := ([max] - [min]) * 0.5 + C1$

Iterate for every (i,j) in I_{smooth} :

$K := (7 \times 7)$ neighbour around each (i,j)
 $\text{thresh2} = \text{mean}(K) + C2$

if $I_{\text{smooth}}[i,j] > \text{thresh2}$
 $I_{\text{smooth}}[i,j] = 255$

else:

$I_{\text{smooth}}[i,j] = 0$

if foreground:

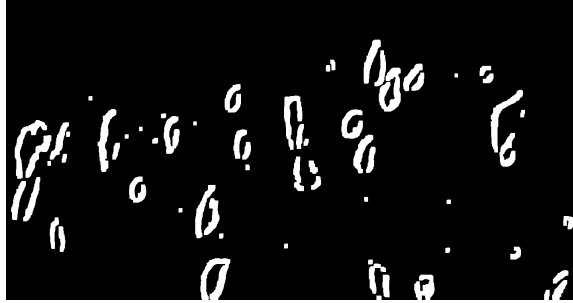
$\text{thresh1}[i] := \text{thresh1}[i] + C3$

Iterate for every pixel in K:

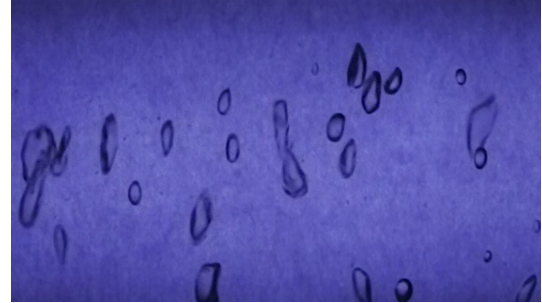
if $K[x,y] - I_{\text{smooth}}[i,j] > \text{thresh}[i]$:
 assign opposite to $I_{\text{smooth}}[i,j]$
else:

assign same to $I_{\text{smooth}}[i,j]$

Perform opening operation on I_{smooth} to get I_{opem}



Segmented Image



Original Image

2. Thinning of edges

For thinning we use the algorithm proposed by Zhang and Suen(Zhang Suen 1984) without any modification. The algorithm is bi-iterative one and uses two different set of conditions to detect boundary pixels.

Steps

Iterate over each (i,j) in I_{opem}

$K := 3 \times 3$ neighbourhood centered at (i,j)

Subiteration 1:

Delete $I_{\text{opem}}(i,j)$ if:

1. $2 \leq B(i,j) \leq 6$
2. $A(i,j) = 1$
3. $K(2)*K(4)*K(6) = 0$
4. $K(4)*K(6)*K(8) = 0$

Subiteration 2:

Delete $I_{\text{opem}}(i,j)$ if:

1. $2 \leq B(i,j) \leq 6$
2. $A(i,j) = 1$
3. $K(2)*K(4)*K(8) = 0$
4. $K(2)*K(6)*K(8) = 0$

Where $B(i,j)$ is the number of non-zero pixel in K other than $I_{open}(i,j)$
 $A(i,j)$ is the number of 0 to 255 transitions in K.

P_9 (i-1,j-1)	P_2 (i-1,j)	P_3 (i-1,j+1)
P_8 (i,j-1)	P_1 (i,j)	P_4 (i,j+1)
P_7 (i+1,j-1)	P_6 (i+1,j)	P_5 (i+1,j+1)

Kernel K



Thinned Image

3 and 4. Unwanted segment removal and marking

As can be seen in the image above the thinned segments have some redundant branches that needs to be removed. Also each of the individual segments are marked for reducing the number of pixels to iterate over in the later stages as well as for grouping of segments.

The logic for branch removal and marking is divided into four separate method.

The logic and code are too complex to explain entirely here so only the outline procedure is given. Please refer to attached code for further clarification

Steps

Iterate over each segment starting from end point:

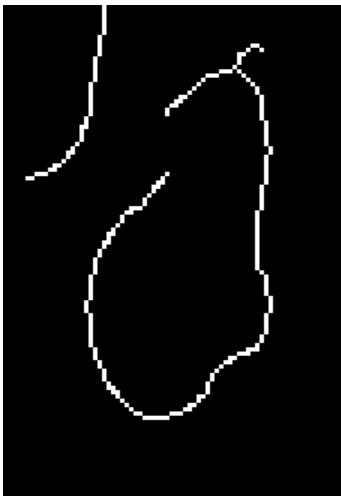
K:=3x3 neighbour with $P_{i,j}$ at centre

s:= Sum(K)

iterate while other endpoint not reached (method mark)

```

if s==1:
    mark pixel
else:
    check if branched (method branches)
    if branched:
        find the longest branch and delete the others (methods which_branch and
        branch_mark)
    
```



With Branch



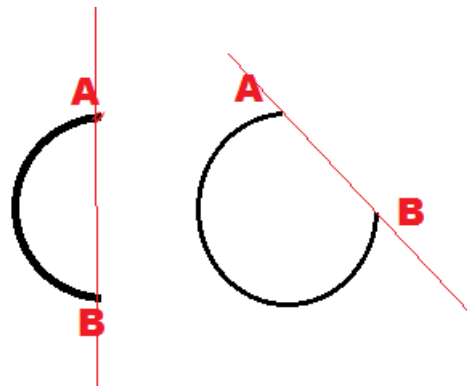
Cleaned

The conditions used for detecting branch-points are as follows:

1. If 2 or more of K[2], K[4], K[6] and K[8] are non-zero the point is branch point,
2. If any two corner pixel are non-zero
3. If any corner pixel and opposite mid-pixel are non zero

Two minor steps follow this step of cleaning and marking, which are determining sufficiently round branches such that they are not considered during grouping and thresholding off segments shorter than 5 pixels in length as minimum of five points are needed to fit an ellipse.

For the first part a simple property of circles is used.



If we observe the two figures, one is a semicircle and other one is a 3/4 circle. If we want to measure the angle covered by each segment then we use the following formulae:

$$\text{Angle covered} = \Theta = (\text{arc length}) / (\text{distance between endpoints})$$

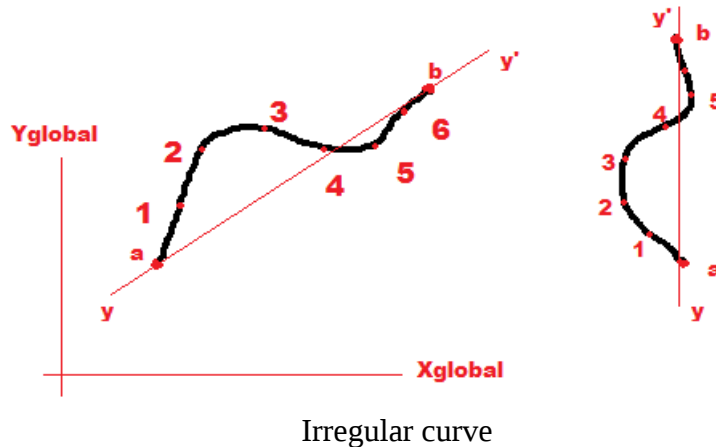
For the first figure $\Theta = 1.57$ and for the second figure $\Theta = 3.33$

So the value of Θ must be more than 1.57 for an arc. We select the value 2 for thresholding closed figures.

5. Convexity based grouping followed by distance based selection

If any closed curve is observed, any portion of it has some convexity. A novel approach of grouping marked segments via convexity matching is used to decide which segments are the neighbouring segments. This approach allows to identify and separate even overlapping bubbles.

We define a new simple measure of convexity and method of finding it.
Consider the irregular arc given below.



We see that the curve can be expressed in global coordinates and also in a local coordinate system whose y axis coincides with the line joining the ends of the curve. On each curve six equidistant points are selected between the end points. Let any point have coordinates (X_G, Y_G) in global coordinates and (X_L, Y_L) in local coordinates. If the point A is (X_a, Y_a) and B is (X_b, Y_b) in global coordinates.

$$\tan(\Theta) = (Y_b - Y_a) / (X_b - X_a)$$

where θ is angle of inclination of the line joining the end points,
Then the transformed coordinates is given by:

$$X_L = X_G * \cos(\Theta) - Y_G * \sin(\Theta)$$

$$Y_L = X_G * \sin(\Theta) + Y_G * \cos(\Theta)$$

The right side figure shows the transformed coordinates. Then we define convexity as follows:

$$\text{Convexity} = \zeta = x_1 + x_2 + x_3 + x_4 + x_5 + x_6$$

For our algorithm the sign of the algorithm is more important than the magnitude.

If end points of the segments be (X_a, Y_a) , (X_b, Y_b) and (X_c, Y_c) , (X_d, Y_d) the sign of the convexity the neighbouring segments are decided by the following rules: (for -ve convexity of AB)

1. If $Y_c > (Y_a \text{ and } Y_b)$ and $Y_d > (Y_a \text{ and } Y_b)$ then if $Y_c > Y_d$ convexity should be positive and if $Y_c < Y_d$ convexity should be negative.
2. If $Y_c > (Y_a \text{ or } Y_b)$ and $Y_d < (Y_a \text{ or } Y_b)$ then convexity should be positive
3. If $Y_c < (Y_a \text{ and } Y_b)$ and $Y_d < (Y_a \text{ and } Y_b)$ then if $Y_c > Y_d$ convexity should be negative and if $Y_c < Y_d$ convexity positive.

If ζ_{AB} and ζ_{CD} be the two convexities then :

$$|\zeta_{AB} - \zeta_{CD}| \leq C_3 \text{ where } C_3 \text{ is between 0 to 2.}$$

After grouping of segments satisfying the convexity requirements distance based thresholding is done such that any curve outside the threshold are neglected.

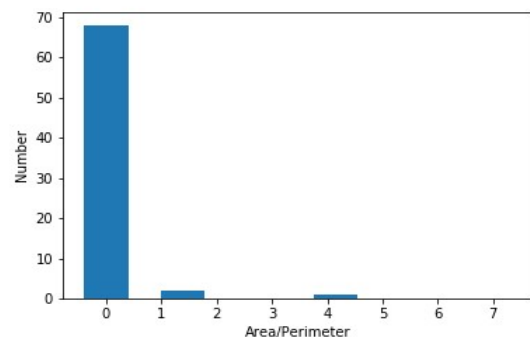
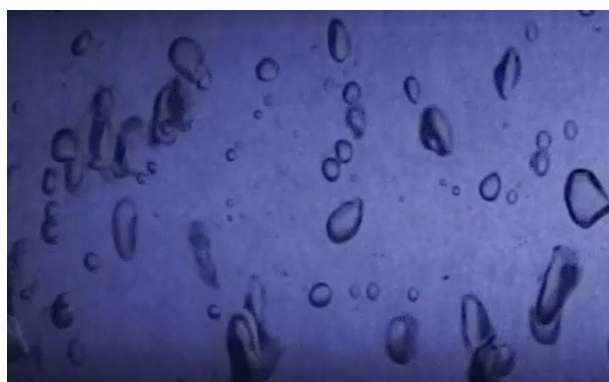
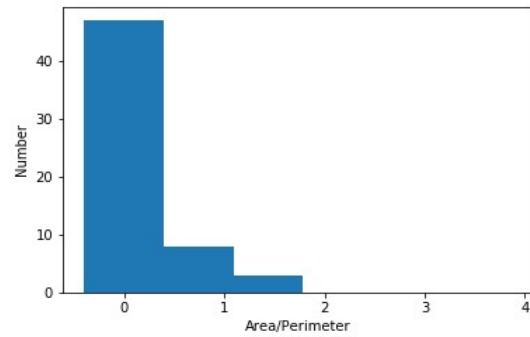
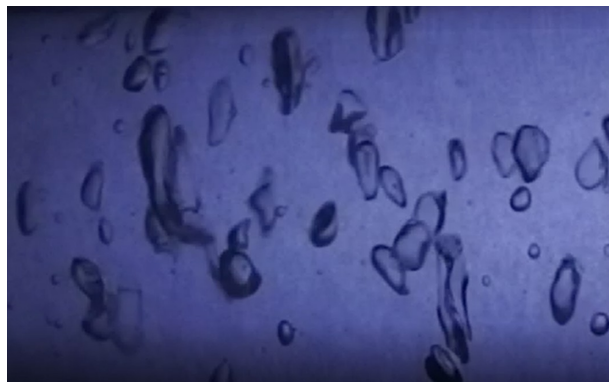
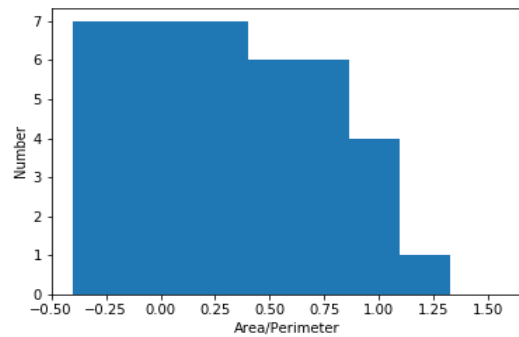
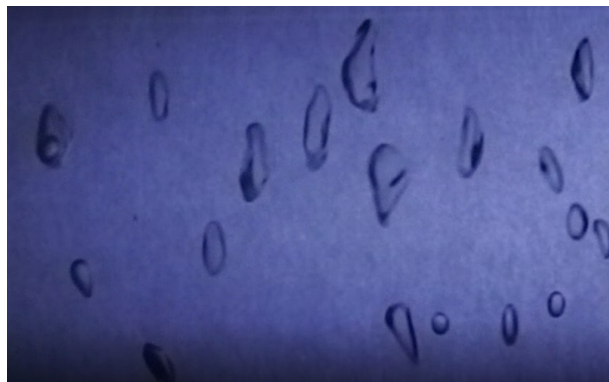
The threshold is taken to be twice the length of the segment from the either end points.

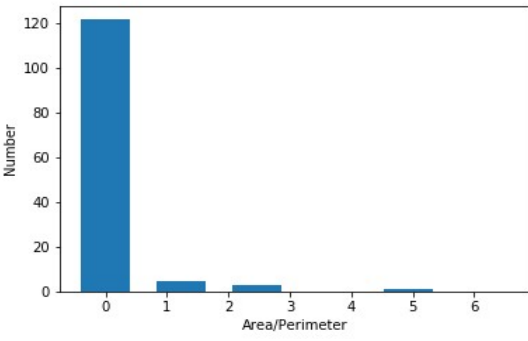
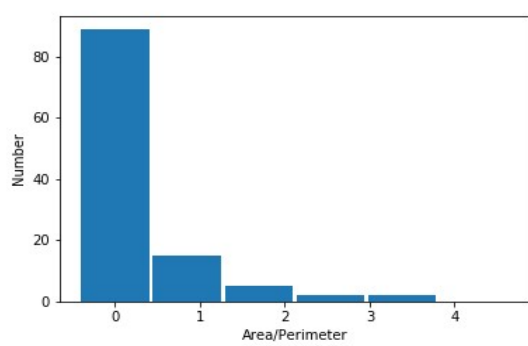
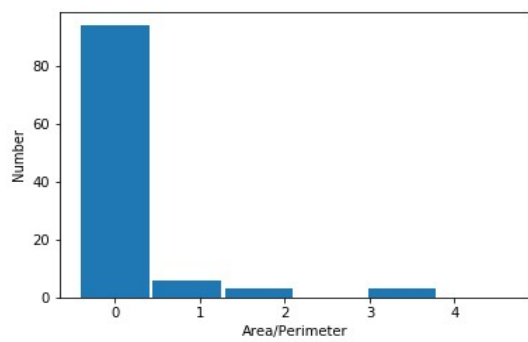
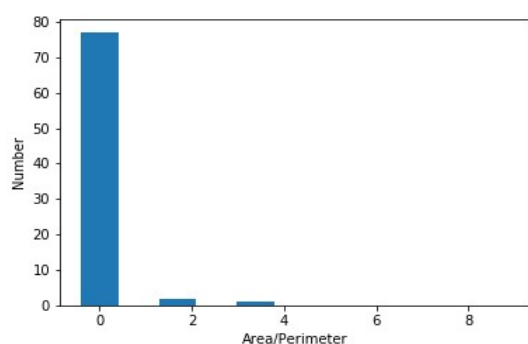
6. Curve Fitting:

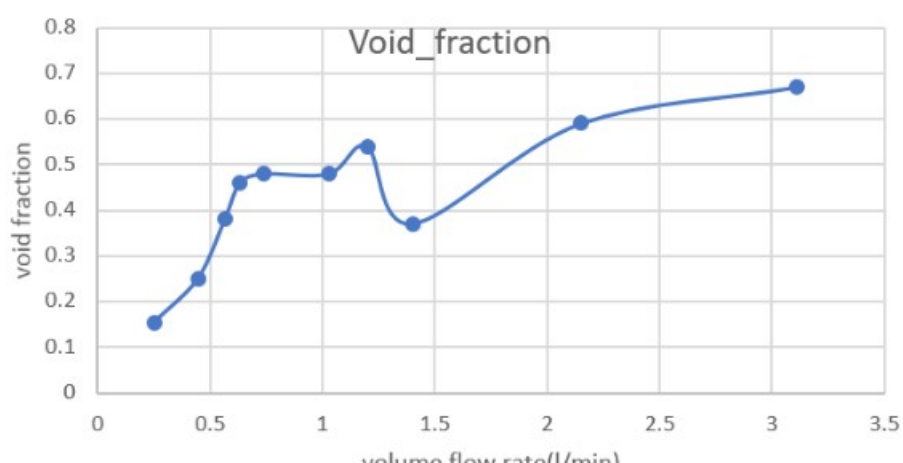
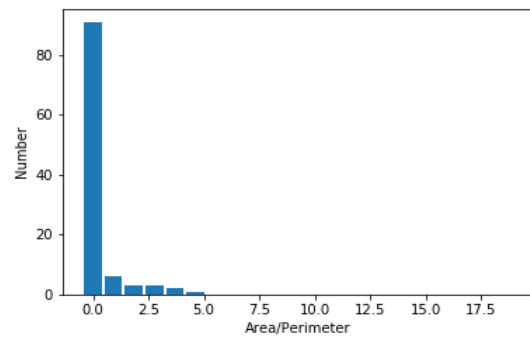
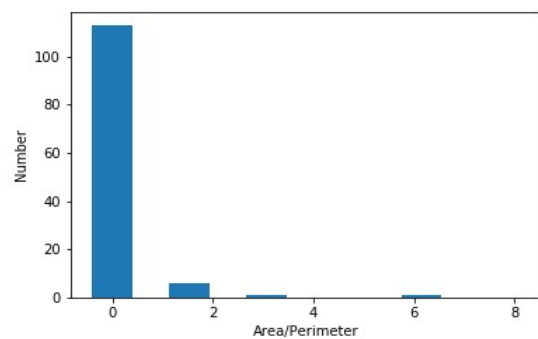
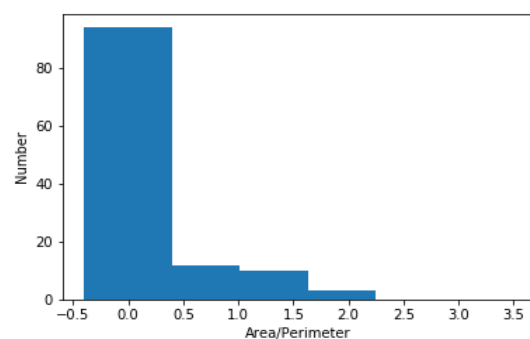
This accomplished by solving simple parametric equation based on all the points and by selecting the minimum fitting ellipse.

The algorithm used is from the paper A Buyer's Guide to Conic Fitting by Fitzggibon and Fisher 1993.

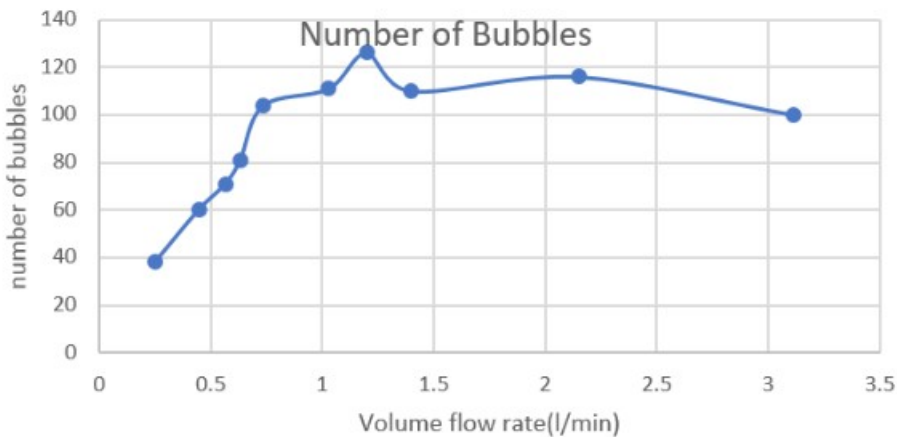
Results and discussion







● Series1



Given above are first the bubble size histogram with volume flow rate. It can be seen as volume flow rate increases in general the number of bubbles first increases to a maximum and then decreases. But the maximum bubble size increases as does the void fraction.

This trend conforms with trends obtained in papers [1],[2]. The bubble flow in bubble columns have two distinct regions-the homogeneous or bubbly flow and the heterogeneous or churn turbulent region. In our experiment the churn turbulent region begins at about 1.04 l/min and the transient region lies beyond .466 l/min. The number of bubbles decrease in higher flow regimes as churn turbulent region begins and smaller bubbles start coalescing into larger bubbles and the number of bubbles decreases. Also the decrease in void fraction at 1.4 is also expected as suddenly many small bubbles coalesce together leading to decrease in total void fraction as surface area decreases.

Conclusion

In this project we developed an algorithm for studying bubble size distribution and void fraction variation with volume flow rate of air. The results produced matches with the results of other papers proving that our algorithm works. There is inaccuracy owing to the fact that image quality was not good and there are scopes of improving the algorithm as well.

Literature Review

1. Omar M Basha; Badie I. Morsi; Novel Approach and Correlation for Bubble Size Distribution in a Slurry Bubble Column Reactor Operating in the Churn-Turbulent Flow Regime ,*Ind. Eng. Chem. Res*,2018
2. Freddy Hernandez-Alvarado; Dinesh V.Kalaga; Damon Turney; Sanjoy Banerjee; B. Joshi; Void fraction, bubble sie and interfacial area measurements in co-current downflow bubble column reactor with microbubble dispersion, *Che. Eng. Sci*, 2017
3. Shahrouz Mohagheghian,etal; Characterization of Bubble Size Distributions within a Bubble Column,*Fluids*,2018
4. Parul Tyagi,etal; Experimental Characterization of Dense Gas-Liquid Flow in a Bubble Column using Voidage Probes, *Che.Eng*,2016
5. Giorgio Besagni,Fabio Inzoli; Bubble size distributions and shapes in annular gap bubble column , *Exp. Thrm. Fld. Sci.*,2015
6. Krushnathej T.S,etal; Experimental studies of bubbly flow in a pseudo-2D micro-structured bubble column reactor using digital image analysis, *Che. Eng. Sci*,2015
7. Ashish Karn,etal; An integrative image measurement technique for dense bubbly flows with a wide size distribution,*Che. Eng. Sci.*;2014
8. Y.M. Lau,etal; Development of an image measurement technique for size distribution in dense bubbly flows, *Che. Eng. Sci*;2013
9. Ugandhar Puli; An image analysis technique for determination of void fraction in subcooled flow boiling of water in horizontal annulus at high pressures, *Int. Jrn. Ht. Ff.*,2012
- 10.. J.G. Daly etal; Measurement of gas holdups and sauter mean bubble diameter in bubble column reactor by dynamic gas disengagement method, *Che. Eng. Sci*,1992